

PAPER

Growth signals determine the topology of evolving networks

To cite this article: Ana Vrani and Marija Mitrovi Dankulov *J. Stat. Mech.* (2021) 013405

View the [article online](#) for updates and enhancements.



IOP | ebooks™

Bringing together innovative digital publishing with leading authors from the global scientific community.

Start exploring the collection—download the first chapter of every title for free.

PAPER: Interdisciplinary statistical mechanics

Growth signals determine the topology of evolving networks

Ana Vranić and Marija Mitrović Dankulov*

Institute of Physics Belgrade, University of Belgrade, Pregreva 118, 11080
Belgrade, Serbia

E-mail: anav@ipb.ac.rs and mitrovic@ipb.ac.rs

Received 2 November 2020

Accepted for publication 15 November 2020

Published 22 January 2021



Online at stacks.iop.org/JSTAT/2021/013405
<https://doi.org/10.1088/1742-5468/abd30b>

Abstract. Network science provides an indispensable theoretical framework for studying the structure and function of real complex systems. Different network models are often used for finding the rules that govern their evolution, whereby the correct choice of model details is crucial for obtaining relevant insights. Here, we study how the structure of networks generated with the aging nodes model depends on the properties of the growth signal. We use different fluctuating signals and compare structural dissimilarities of the networks with those obtained with a constant growth signal. We show that networks with power-law degree distributions, which are obtained with time-varying growth signals, are correlated and clustered, while networks obtained with a constant growth signal are not. Indeed, the properties of the growth signal significantly determine the topology of the obtained networks and thus ought to be considered prominently in models of complex systems.

Keywords: random graphs, networks, network dynamics, stochastic processes

 Supplementary material for this article is available [online](#)

J. Stat. Mech. (2021) 013405

Contents

1. Introduction	2
2. Growth signals	3

*Author to whom any correspondence should be addressed.

3. Model of aging nodes with time-varying growth	6
4. Structural differences between networks generated with different growth signals	7
5. Discussion and conclusions	12
Acknowledgments	13
References	14

1. Introduction

Emergent collective behavior is an indispensable property of complex systems [1]. It occurs as a consequence of interactions between a large number of units that compose a complex system, and it cannot be easily predicted from the knowledge about the behavior of these units. The previous research offers definite proof that the interaction network structure is inextricably associated with the dynamics and function of the complex system [2–9]. The structure of complex networks is essential for understanding the evolution and function of various complex systems [10–13].

The structure and dynamics of real complex systems are studied using complex network theory [1, 10, 11]. It was shown that real networks have similar topological properties regardless of their origins [14]. They have broad degree distribution, degree–degree correlations, and power-law scaling of clustering coefficient [11, 14]. Understanding how these properties emerge in complex networks leads to the factors that drive their evolution and shape their structure [2].

The complex network models substantially contribute to our understanding of the connection between the network topology and system dynamics and uncover underlying mechanisms that lead to the emergence of distinctive properties in real complex networks [15–17]. For instance, the famous Barabási–Albert model [15] finds the emergence of broad degree distribution to be a consequence of preferential attachment and network growth. Degree–degree anti-correlations of the internet can be explained, at least to a certain extent, by this constraint [18, 19]. Detailed analysis of the emergence of clustered networks shows that clustering is either the result of finite memory of the nodes [20] or occurs due to triadic closure [21].

Network growth, in combination with linking rules, shapes the network topology [22]. While various rules have been proposed to explain the topology of real networks [10], most models assume a constant rate of network growth, i.e., the addition of a fixed number of nodes at each time step [15, 20, 21]. However, empirical analysis of numerous technological and social systems shows that their growth is time-dependent [23–26]. The time-dependent growth of the number of nodes and links in the networks has been considered as a parameter in uncovering network growth mechanisms [27]. The accelerated growth of nodes in complex networks is the cause of the high heterogeneity in the distribution of web pages among websites [23] and the emergence of highly cited authors in citation networks [26]. The accelerated growth of the number of new links added in each time step changes the shape and scaling exponent of degree distribution

in the Barabási–Albert model [28] and model with preferential attachment with aging nodes [29].

The growth of real systems is not always accelerated. The number of new nodes joining the system varies in time, has trends, and exhibits circadian cycles typical for human behavior [24, 25, 30]. These signals are multifractal and have long-range correlations [31]. Some preliminary evidence shows that the time-varying growth influences the structure and dynamics of the social system and, consequently, the structure of interaction networks in social systems [25, 30, 32–34]. Still, which properties of the real growth signal have the most considerable influence, how different properties influence the topology of the generated networks, and to what extent is an open question.

In this work, we explore the influence of real and computer-generated time-varying growth signals on complex networks' structural properties. We adapt the aging nodes model [35] to enable time-varying growth. We compare the networks' structure using the growing signals from empirical data and randomized signals with ones grown with the constant signal using D -measure [36]. We demonstrate that the growth signal determines the structure of generated networks. The networks grown with time-varying signals have significantly different topology compared to networks generated through constant growth. The most significant difference between topological properties is observed for the values of model parameters for which we obtain networks with broad degree distribution, a common characteristic of real networks [10]. Our results show that real signals, with trends, cycles, and long-range correlations, alter networks' structure more than signals with short-range correlations.

This paper is divided as follows. In section 2, we provide a detailed description of growth signals. In section 3, we briefly describe the original model with aging nodes and structural properties of networks obtained for different values of model parameters [35]. We also describe the changes in the model that we introduce to enable time-varying growth. We describe our results in section 4 and show that the values of D -measure indicate large structural differences between networks grown with fluctuating and ones grown with constant signals. This difference is particularly evident for networks with power-law degree distribution and real growth signals. The networks generated with real signals are correlated and have hierarchical clustering, properties of real networks that do not emerge if we use constant growth. We discuss our results and give a conclusion in section 5.

2. Growth signals

The *growth signal* is the number of new nodes added in each time step. Real complex networks evolve at a different pace, and the dynamics of link creation define the time unit of network evolution. For instance, the co-authorship network grows through establishing a link between two scientists when they publish a paper [37]. In contrast, the links in an online social network are created at a steady pace, often interrupted by sudden bursts [38]. A paper's publication is thus a unit of time for the evolution of co-authorship networks, while the most appropriate time unit for social networks is 1 min or 1 h. While systems may evolve at a different pace, their evolution is often driven by the related mechanisms reflected by the similarity of their structure [10].

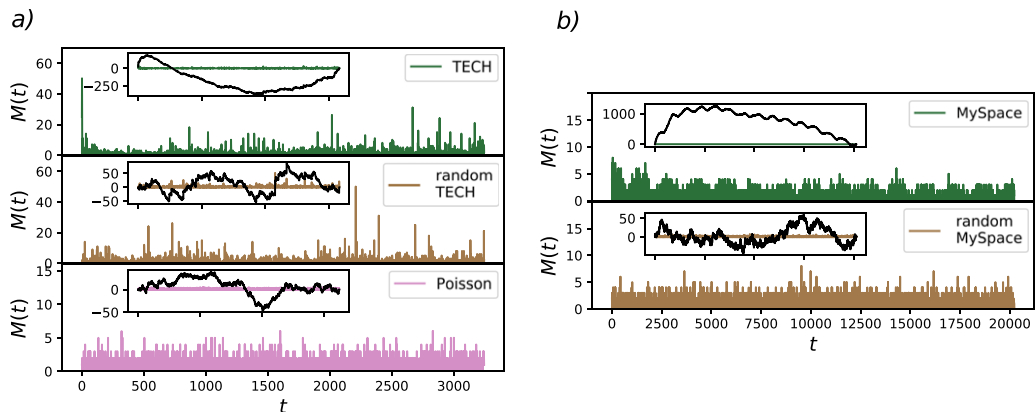


Figure 1. Growth signals for TECH (a) and MySpace (b) social groups, their randomized counterparts, and random signal drawn from Poissonian distribution with mean 1. The cumulative sums of signals' deviations from average mean value are shown in insets.

In this work, we use two different growth signals from real systems figure 1: (a) the data set from TECH community from Meetup social website [39] and (b) two months dataset of MySpace social network [40]. TECH is an event-based community where members organize offline events through the Meetup site [39]. The time unit for TECH is event since links are created only during offline group meetings. The growth signal is the number of people that attend the group's meetings for the first time. MySpace signal shows the number of new members occurring for the first time in the dataset [40] with a time resolution of 1 min. The number of newly added nodes for the TECH signal is $N = 3217$, and the length of the signal is $T_s = 3162$ steps. We have shortened the MySpace signal to $T_s = 20\,221$ time steps to obtain the network with $N = 10\,000$ nodes. The signals in the inset of figures 1(a) and (b) show the cumulative sum of deviations of signals from their average mean value, which is 1.017 for TECH and random TECH signal, 0.47 for MySpace and random MySpace, and 1 for Poissonian signal.

Real growth signals have long-range correlations, trends and cycles [25, 30, 40]. We also generate networks using randomized signals and one computer-generated white-noise signal to explore the influence of signals' features on evolving networks' structure. We randomize real signals using a reshuffling procedure. The reshuffling procedure consists of E steps. We randomly select two signal values at two distinct time steps and exchange their position in each step. The number of reshuffling steps is proportional to the length of the signal T_s , and in our case, it equals $100T_s$. Using this procedure, we keep the signal length and mean value, the number of added nodes, and the probability density function of fluctuations intact, but destroy cycles, trends, and long-range correlations. Besides, we generate a white-noise signal from a Poissonian probability distribution with a mean equal to 1. The length of the signal is $T = 3246$, and the number of added nodes in the final network is the same as for the TECH signal.

We characterize the long-range correlations of the growth signals calculating Hurst exponent [41, 42]. Hurst exponent describes the scaling behavior of time series $M(xt) = x^H M(t)$. It takes values between 0.5 and 1 for long-range correlated signals

and $H = 0.5$ for short-range correlated signals. The most commonly used method for estimating Hurst exponent of real, often non-stationary, temporal signals is detrended fluctuation analysis (DFA) [41]. The DFA removes trends and cycles of real signals and estimates Hurst exponent based on residual fluctuations. The DFA quantifies the scaling behavior of the second-moment fluctuations. However, signals can have deviations in fractal structure with large and small fluctuations that are characterized by different values of Hurst exponents [31].

We use multifractal detrended fluctuation analysis (MFDFA) [31, 43] to estimate multifractal Hurst exponent $H(q)$. For a given time series $\{x_i\}$ with length N , we first define global profile in the form of cumulative sum equation (1), where $\langle x \rangle$ represents an average of the time series:

$$Y(j) = \sum_{i=0}^j (x_i - \langle x \rangle), \quad j = 1, \dots, N. \quad (1)$$

Subtracting the mean of the time series is supposed to eliminate global trends. Insets of figure 1 show global profiles of TECH, MySpace, their randomized signals and Poissonian distribution. The profile of the signal Y is divided into $N_s = \text{int}(N/s)$ non overlapping segments of length s . If N is not divisible with s the last segment will be shorter. This is handled by doing the same division from the opposite side of time series which gives us $2N_s$ segments. From each segment ν , local trend $p_{\nu,s}^m$ —polynomial of order m —should be eliminated, and the variance $F^2(\nu, s)$ of detrended signal is calculated as in equation (2):

$$F^2(\nu, s) = \frac{1}{s} \sum_{j=1}^s [Y(j) - p_{\nu,s}^m(j)]^2. \quad (2)$$

Then the q th order fluctuating function is:

$$F_q(s) = \left\{ \frac{1}{2N_s} \sum_{\nu}^{2N_s} [F^2(\nu, s)]^{\frac{q}{2}} \right\}^{\frac{1}{q}}, \quad q \neq 0 \quad (3)$$

$$F_0(s) = \exp \left\{ \frac{1}{4N_s} \sum_{\nu}^{2N_s} \ln [F^2(\nu, s)] \right\}, \quad q = 0.$$

The fluctuating function scales as power-law $F_q(s) \sim s^{H(q)}$ and the analysis of log–log plots $F_q(s)$ gives us an estimate of multifractal Hurst exponent $H(q)$. Multifractal signal has different scaling properties over scales while monofractal is independent of the scale, i.e., $H(q)$ is constant.

Figures 1(a) and 2 show that the TECH signal has long trends and a broad probability density function of fluctuations. The trends are erased from the randomized TECH signal, but the broad distribution of the signal and average value remain intact. MFDFA analysis shows that real signals have long-range correlations with Hurst exponent approximately 0.6 for $q = 2$, figure 2. The TECH signal is multifractal, resulting from both broad probability distribution for the values of time series and different long-range correlations of the intervals with small and large fluctuations. Reshuffling of the

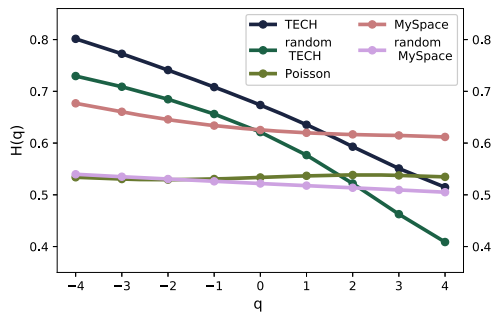


Figure 2. Dependence of Hurst exponent on parameter q for all five signals shown in figure 1 obtained with MF DFA.

time series does not destroy the broad distribution of values, which is the cause for the persistent multifractality of the TECH randomized signal is figure 2.

MySpace signal has a long trend with additional cycles that are a consequence of human circadian rhythm, figure 1(b). Circadian rhythm is an internal process that regulates the sleep-wake cycle and activity, and its period for humans is 24 h [44]. Circadian rhythm leads to periodic changes in online activity during the day and the emergence of a well-defined daily rhythm of activity that we see in figure 1(b). MySpace signal is multifractal for $q < 0$, and has constant value of $H(q)$ for $q > 0$, figure 2. In MF DFA, with negative values of q , we emphasize segments with smaller fluctuations, while for positive q , the emphasis is more on segments with larger fluctuations [43]. Segments with smaller fluctuations have more persistent long-range correlations in both real signals, see figure 2. Randomized MySpace signal and Poissonian signal are monofractal and have short-range with $H = 0.5$ correlations typical for white noise.

Detailed MDFA analysis of real, shuffled, and computer-generated signals are shown in figure S1 and table S1 of the supplementary material (<https://stacks.iop.org/JSTAT/2021/013405/mmedia>). In figure S1 we show in details how the $F_q(s)$ depends on s for different values of parameter q . The curve $F_q(s)$ exhibits different slopes for different values of q for multifractal signals, i.e., TECH, random TECH, and MySpace. $F_q(s)$ curves for monofractal signals are parallel. We provide the estimated values of $H(q)$ with estimated errors for q in a range from -4 to 4 for all five signals in table S1 of the supplementary material.

3. Model of aging nodes with time-varying growth

To study the influence of temporal fluctuations of growth signal on network topology, we need a model with linking rules where linking probability between network nodes depends on time. We use a network model with aging nodes [35]. In this model, the probability of linking the newly added node and the old one is proportional to their age difference and an old node's degree. In the original version of the model, one node is added to the network and linked to one old node in each time step. The old node is

chosen according to probability

$$\Pi_i(t) \sim k_i(t)^\beta \tau_i^\alpha \quad (4)$$

where $k_i(t)$ is a degree of a node i at time t , and τ_i is age difference between node i and newly added node. As was shown in [35], the values of model parameters β and α determine the topological properties of the resulting networks grown with the constant signal. According to this work, the networks generated using constant growth signals are uncorrelated trees for all values of model parameters. The phase diagram in α - β plain, obtained for $\beta > 0$ and $\alpha < 0$, shows that the degree distribution $P(k) \sim k^{-\gamma}$ with $\gamma = 3$ is obtained only along the line $\beta(\alpha^*)$, see [35] and figure S2 in the supplementary material. For $\alpha > \alpha^*$ networks have gel-like small world behavior, while for $\alpha < \alpha^*$ but close to line $\beta(\alpha^*)$ networks have stretched exponential shape of degree distribution [35].

Here we slightly change the original aging model [35] to enable the addition of more than one node and more than one link per newly added node in each time step. In each time step, we add $M \geq 1$ new nodes to the network and link them to $L \geq 1$ old nodes according to probability Π_i given in equation (4). Again, the networks with broad degree distribution are only generated for the combination of the model parameters along the critical line $\beta(\alpha^*)$. This line's position in the α - β plane changes with link density, while the addition of more than one node in each time step does not influence its position. Our analysis shows that the critical line's position is independent of the growth signal's properties, see figure S2 in the supplementary material showing phase diagram. For instance, for $L = 1$ networks and $\alpha = -1.25$ and $\beta = 1.5$ we obtain networks with power-law degree, while for $L = 2$ and $\beta = 1.5$ we need to increase the value of parameter α to -1.0 in order to obtain networks with broad degree distribution. Networks obtained for the values of model parameters $\beta(\alpha^*)$, $L \geq 2$, and constant growth have power-law degree distribution, are uncorrelated and have a finite non-zero value of clustering coefficient which does not depend on node degree, figure 4(b). If we fix the value of parameter β and lower down the value of parameter α to -1.5 , the resulting networks are uncorrelated with a small value of clustering coefficient, see figure 4(a). For $\alpha < \alpha^*$ we obtain networks with stretched exponential degree distribution, without degree-degree correlations and small value of clustering exponent that does not depend on node degree (see figure S2 in the supplementary material). For $\alpha \ll \alpha^*$ the resulting networks are regular graphs. If we keep the value of α to 1.0 but increase the value β to 2.0 we enter the region of small world gels, see figure 4(c). The networks created for the values of $\alpha > \alpha^*$ are correlated networks with power-law dependence of the clustering coefficient on the degree (see figure S2 in the supplementary material). However, these networks do not have a power-law degree distribution.

The master equation approach is useful for studying the model with aging nodes when $M(t) = 1$ [45]. However, this approach is not sufficient for time-varying growth signals. In this work, we use numerical simulations to explore the case when $M(t)$ is a correlated time-varying function and study how these properties influence the structure of generated networks for different values of parameter $-\infty < \alpha \leq 0$ and $\beta \geq 1$ and constant L .

4. Structural differences between networks generated with different growth signals

We generate networks for different values of L , and different growth signal profiles $M(t)$. To examine how these properties influence the network structure, we compare the network structure obtained with different growth signals with networks of the same size grown with constant signal $M = 1$. The $M = 1$ is the closest constant value to average values of the signals, which are 1.017 for TECH, 0.47 for MySpace, and 1 for Poissonian signals. We explore the parameter space of the model by generating networks for pairs of values (α, β) in the range $-3 \leq \alpha \leq -0.5$ and $1 \leq \beta \leq 3$ with steps 0.5. For each pair of (α, β) we generated networks of different link density by varying parameter $L \in 1, 2, 3$, and for each combination of (α, β, L) , we generate a sample of 100 networks and compare the structure of the networks grown with $M = 1$ with the ones grown with $M(t)$ shown in figure 1.

We quantify topological differences between two networks using D -measure defined in [36]

$$D(G, G') = \omega \left| \sqrt{\frac{J(P_1, \dots, P_N)}{\log(d+1)}} - \sqrt{\frac{J(P'_1, \dots, P'_N)}{\log(d'+1)}} \right| + (1 - \omega) \sqrt{\frac{J(\mu_G, \mu_{G'})}{\log 2}}. \quad (5)$$

D -measure captures the topological differences between two networks, G and G' , on a local and global level. The first term in equation (5) evaluates dissimilarity between two networks on a local level. For each node in the network G one can define the distance distribution $P_i = \{p_i(j)\}$, where $p_i(j)$ is a fraction of nodes in network G that are connected to node i at distance j . The set of N node-distance distributions $\{P_1, \dots, P_N\}$ contains a detailed information about network's topology. The heterogeneity of a graph G in terms of connectivity distances is measured through node network dispersion (NND). In [36] authors estimate NND as Jensen–Shannon divergence between N distance distributions $J(P_1, \dots, P_N)$ normalized by $\log(d+1)$, where d is diameter of network G , and show that NND captures relevant features of heterogeneous networks. The difference between NNDs for graph G and G' captures the dissimilarity between the graph's connectivity distance profile.

However, certain graphs, such as k -regular graphs, have $\text{NND} = 0$ and can not be compared using NND. For these reasons, authors also introduce average node distance distribution of a graph $\mu(G) = \{\mu(1), \dots, \mu(d)\}$, where $\mu(k)$ is the fraction of all pair of nodes in the network G that are at a distance k . The Jensen–Shannon divergence between $\mu(G)$ and $\mu(G')$ measures the difference between nodes' average connectivity in a graph G and G' . This term captures the differences between nodes on a global scale.

The original definition of D -measure also includes the third term, which quantifies dissimilarity in node α -centrality. The term can be omitted without precision loss [36]. The parameter ω in equation (5) determines the weight of each term. The extensive analysis shows that the choice $\omega = 0.5$ is the most appropriate for quantifying structural differences between two networks [36].

The D -measure takes the value between 0 and 1. The lower the value of D -measure is the more similar two networks are, with $D = 0$ for isomorphic graphs. The D -measure

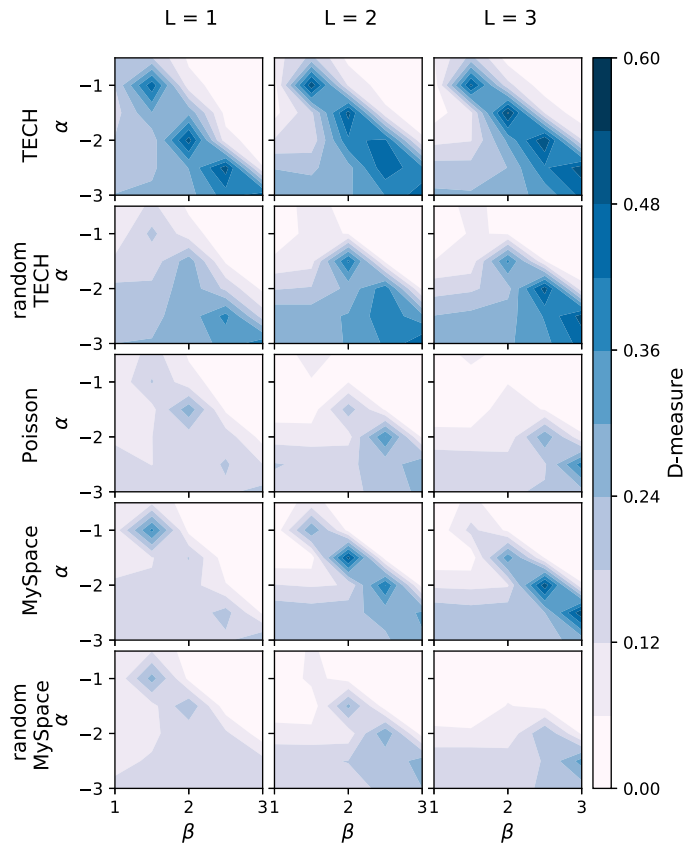


Figure 3. The comparison of networks grown with growth signals shown in figure 1 versus ones grown with constant signal $M = 1$, for value of parameter $\alpha \in [-3, -1]$ and $\beta \in [1, 3]$. $M(t)$ is the number of new nodes, and L is the number of links added to the network in each time step. The compared networks are of the same size.

outperforms previously used network dissimilarity measures such as Hamming distance and graph editing distance and clearly distinguishes between networks generated with the same model but with different values of model parameters [36].

For each pair of networks, one grown with constant and one with the fluctuating signal, we calculate the D -measure. The structural difference between networks grown with constant and fluctuating growth signal for fixed L and values of parameters α and β is obtained by averaging the D -measure calculated between all possible pairs of networks, see figure 3. We observe the non-zero value of D -measure for all time-varying signals. The D -measure has the largest value in the region around the line $\beta(\alpha^*)$. The values of D -measure in this region are similar to ones observed when comparing Erdős–Rényi graphs grown with linking probability below and above critical value [36]. For values $\beta < \beta(\alpha^*)$, the structural differences between networks grown with constant signal and $M(t)$ still exist, but they become smaller as we are moving away from the critical line. Networks obtained with constant signal and fluctuating signals have statistically similar structural properties in the region of small-world network gels, i.e., $\alpha > \alpha^*$.

We focus on the region around the critical line and observe the significant structural discrepancies between networks created for constant versus time-dependent growth signals for all signals regardless of their features. However, the value of D -measure depends on the signal's properties, figure 3. Networks grown with multifractal signals, TECH, random TECH, and MySpace signals, are the most different from those created by a constant signal. The D -measure has the maximum value for the original TECH signal, with $D_{\max} = 0.552$, the signal with the most pronounced multifractal properties among all signals shown in figure 2. Networks generated with randomized MySpace signal and Poisson signal are the least, but still notably dissimilar from those created with $M = 1$.

Randomized MySpace signal and Poissonian signal are monofractal signals with Hurst exponent $H = 0.5$. To investigate the influence of monofractal correlated signals on the network structure, we generate six signals with a different value of $H \in \{0.5, 0.6, 0.7, 0.8, 0.9, 1.0\}$, see figure S3 in the supplementary material. We use each of these signals to generate networks following the same procedure as for signals shown in figure 1. The results shown in figure S4 of the supplementary material confirm that short-range correlated signals create networks with different structures from ones grown with the constant signal. The increase of the Hurst exponent leads to increases in the D -measure. However, D -measure's maximal value is smaller than one observed for multifractal signals shown in figure 3.

The value of D -measure rises with a decline of α^* . This observation can be explained by examining linking rules and how model parameters determine linking dynamics between nodes. The ability of a node to acquire a link declines with its age and grows with its degree. A node's potential to become a hub, node with a degree significantly larger than average network degree, depends on the number of nodes added to the network in the T time steps after its birth. The length of the interval T decreases with parameter α . For constant signal, the number of nodes added during this time interval is constant and equal to MT . For fluctuating growth signals, the number of added nodes during the time T varies with time. In signals that have a broad distribution of fluctuations, like TECH signals, the peaks of the number of newly added nodes lead to the emergence of one or several hubs and super hubs. The emergence of super hubs, nodes connected to more than 30% of the nodes in the network, significantly alters the network's topology. For instance, super hubs' existence lowers the value of average path length and network diameter [10]. The emergence of hubs occurs for values of parameter α relative close to -1.0 for signals with long-range correlations. As we decrease the parameter α , the fluctuations present in the time-varying signals become more important, and we observe the emergence of hubs even for the white-noise signals. The trends present in real growth signals further promote the emergence of hubs. The impact of fluctuations and their temporal features on the structure of complex networks increases with link density.

The large number of structural properties observed in real networks are often consequences of particular degree distributions, degree correlations, and clustering coefficient [47]. Figure 4 shows the degree distribution $P(k)$, dependence of average neighboring degree on node degree $\langle k \rangle_{nn}(k)$, and dependence of clustering coefficient on node degree $c(k)$ for networks with average number of links per node $L = 2$. The significant structural differences between networks grown with real time-varying and constant signals

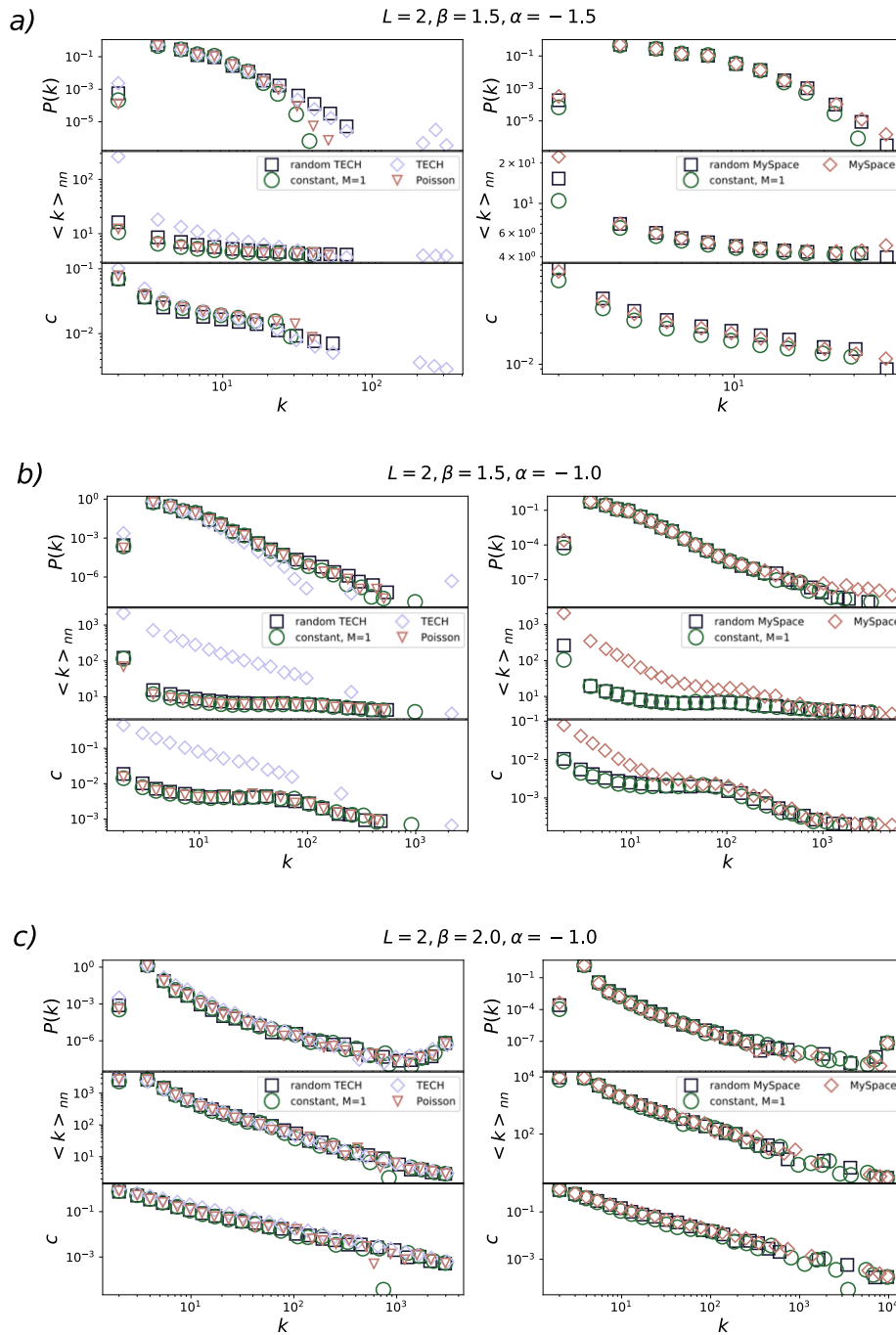


Figure 4. Degree distribution, the dependence of average first neighbor degree on node degree, dependence of node clustering on node degree for networks grown with different time-varying and constant signals. Model parameters have the values $\alpha = -1.5$, $\beta = 1.5$ (a), $\alpha = -1.0$, $\beta = 1.5$ (b), $\alpha = -1.0$, $\beta = 2.0$ (c), and $L = 2$ for all networks.

are observed for the values of model parameters $\alpha = -1.0$ and $\beta = 1.5$, figures 3 and 4(b). The degree distribution of networks generated for real signals shows the occurrence of super hubs in these networks. In contrast, degree distributions of networks generated with white-noise like signals do not differ from one created with constant signal, figure 4(b). Networks obtained for the real signals are disassortative and have a hierarchical structure, i.e., their clustering coefficient decreases with the degree. On the other hand, networks generated with constant and randomized signals are uncorrelated, and their clustering weakly depends on the degree.

We observe a much smaller, but still noticeable, difference between the topological properties of networks evolved with constant and time-varying signal for $\alpha < \alpha^*$, figure 4(a). The difference is particularly observable for degree distribution and dependence of average neighboring degree on node degree of networks grown with real TECH signal. The fluctuations of time-varying growth signals do not influence the topological properties of small-world gel networks, figure 4(c). For $\alpha > \alpha^*$, the super hubs emerge even with the constant growth. Since this is the mechanism through which the fluctuations alter the structure of evolving networks for $\alpha \leq \alpha^*$, the features of the growth signals cease to be relevant.

5. Discussion and conclusions

We demonstrate that the resulting networks' structure depends on the time-varying signal features that drive their growth. The previous research [25, 30] indicated the possible influence of temporal fluctuations on network properties. Our results show that growth signals' temporal properties generate networks with power-law degree distribution, non-trivial degree–degree correlations, and clustering coefficient even though the local linking rules, combined with constant growth, produce uncorrelated networks for the same values of model parameters [35].

We observe the most substantial dissimilarity in network structure along the critical line, the values of model parameters for which we generate broad degree distribution networks. Figure 3 shows that dissimilarity between networks grown with time-varying signals and ones grown with constant signals always exists along this line regardless of the features of the growth signal. However, the magnitude of this dissimilarity strongly depends on these features. We observe the largest structural difference between networks grown with multifractal TECH signal and networks that evolve by adding one node in each time step. The identified value of D -measure is similar to one calculated in the comparison between sub-critical and super-critical Erdős–Rényi graphs [36] indicating the considerable structural difference between these networks. Our findings are further confirmed in figure 4(b). The networks generated with signals with trends and long-range temporal correlations differ the most from those grown with the constant signal. Our results show that even white-noise type signals can generate networks significantly different from ones created with constant signal for low values of α^* .

Randomized and computer-generated signals do not have trends or cycles. Nevertheless, networks grown with these signals have a significantly different structure from ones grown with constant M . Our results demonstrate that growth signals' temporal

fluctuations are the leading cause for the structural differences between networks evolved with the constant and time-varying signal. We observe the smallest, but significant, difference between networks generated with constant M and monofractal signal with short-range correlations. As we increase the Hurst exponent, the value of the D -measure increases. The most considerable differences are observed for multifractal signals TECH, random TECH, and MySpace.

The value of D -measure declines as we move away from the critical line, figure 3. The primary mechanism through which the fluctuations influence the structure of evolved networks is the emergence of hubs and super hubs. For values of $\alpha \ll \alpha^*$, the nodes attach to their immediate predecessors creating regular networks without hubs. For $\alpha \lesssim \alpha^*$ graphs have stretched exponential degree distribution with low potential for the emergence of hubs. Still, multifractal signal TECH enables the emergence of hub even for the values of parameters for which we observe networks with stretched-exponential degree distribution in the case of constant growth figure 4(a). By definition, small-world networks generated for $\alpha > \alpha^*$ have super-hubs [35] regardless of the growth signal. Therefore the effects that fluctuations produce in the growth of networks do not come to the fore for values of model parameters in this region of α - β plane.

In this work, we focus on the role of the node growth signal in evolving networks' structure. However, real networks do not evolve only due to the addition of new nodes, but also through addition of new links [27–29, 38]. Furthermore, the deactivation of nodes [48] and the links [48] influence the evolving networks' structure. Each of these processes alone can result in a different network despite having the same linking rules. The next step would be to examine how different combinations of these processes influence the evolving networks' structure. For instance, in [28], authors have examined the influence of the time-dependent number of added links $L(t)$ on the Barabási–Albert networks' structure. They show that as long as the average value of time-dependent signal $\langle L(t) \rangle$ is independent of time, the generated networks have a similar structure as Barabási–Albert networks, and that the degree distribution depends strongly on the behavior of $\langle L(t) \rangle$. It would be interesting to examine how correlated $L(t)$ signals influence networks' structure with aging nodes, where the age of a node plays a vital role in linking between new and old nodes. Moreover, we expect that the combination of time-varying growth of the number of nodes and the number of links will significantly influence these networks' structure.

Evolving network models are an essential tool for understanding the evolution of social, biological, and technological networks and mechanisms that drive it [10]. The most common assumption is that these networks evolve by adding a fixed number of nodes in each time step [10]. So far, the focus on developing growing network models was on linking rules and how different rules lead to networks of various structural properties [10]. Growth signals of real systems are not constant [25, 30]. They are multifractal, characterised with long-range correlations [25], trends and cycles [40]. Research on temporal networks has shown that temporal properties of edge activation in networks and their properties can affect the dynamics of the complex system [12]. Our results imply that modeling of social and technological networks should also include non-constant growth. Its combination with local linking rules can significantly alter the structure of generated networks.

Acknowledgments

We acknowledge funding provided by the Institute of Physics Belgrade, through the grant by the Ministry of Education, Science, and Technological Development of the Republic of Serbia. This research was supported by the Science Fund of the Republic of Serbia, 65241005, AI-ATLAS. Numerical simulations were run on the PARADOX-IV supercomputing facility at the Scientific Computing Laboratory, National Center of Excellence for the Study of Complex Systems, Institute of Physics Belgrade. The work of MMD was, in part, supported by the Ito Foundation fellowship.

References

- [1] Ladyman J, Lambert J and Wiesner K 2013 What is a complex system? *Euro J. Phil. Sci.* **3** 33
- [2] Barrat A, Barthelemy M and Vespignani A 2008 *Dynamical Processes on Complex Networks* (Cambridge: Cambridge University Press)
- [3] Pascual M *et al* 2006 *Ecological Networks: Linking Structure to Dynamics in Food Webs* (Oxford: Oxford University Press)
- [4] Castellano C, Fortunato S and Loreto V 2009 Statistical physics of social dynamics *Rev. Mod. Phys.* **81** 591
- [5] Gosak G, Markovič R, Dolensek J, Rupnik M S, Marhl M, Stožer A and Perc M 2018 Network science of biological systems at different scales: a review *Phys. Life Rev.* **24** 118–35
- [6] Arenas A, Díaz-Guilera A, Kurths J, Moreno Y and Zhou C 2008 Synchronization in complex networks *Phys. Rep.* **469** 93
- [7] Boccaletti S, Almendral J A, Guan S, Leyva I, Liu Z, Sendiña-Nadal I, Wang Z and Zou Y 2016 Explosive transitions in complex networks' structure and dynamics: percolation and synchronization *Phys. Rep.* **660** 1
- [8] Chen H, Zhang H and Shen C 2018 Double phase transition of the Ising model in core-periphery networks *J. Stat. Mech.* **063402**
- [9] Kuga K and Tanimoto J 2018 Impact of imperfect vaccination and defense against contagion on vaccination behavior in complex networks *J. Stat. Mech.* **113402**
- [10] Boccaletti S, Latora V, Moreno Y, Chavez M and Hwang D 2006 Complex networks: structure and dynamics *Phys. Rep.* **424** 175
- [11] Newman M E J 2010 *Networks: An Introduction* (Oxford: Oxford University Press)
- [12] Holme P and Saramäki J 2012 Temporal networks *Phys. Rep.* **519** 97
- [13] Boccaletti S, Bianconi G, Criado R, Del Genio C I, Gómez-Gardeñes J, Romance M, Sendiña-Nadal I, Wang Z and Zanin M 2014 The structure and dynamics of multilayer networks *Phys. Rep.* **544** 1
- [14] Barabási A-L 2009 Scale-free networks: a decade and beyond *Science* **325** 412
- [15] Barabási A-L and Albert R 1999 Emergence of scaling in random networks *Science* **286** 509
- [16] Tadić B 2001 Dynamics of directed graphs: the world-wide web *Physica A* **293** 273
- [17] Mitrović M and Tadić B 2009 Spectral and dynamical properties in classes of sparse networks with mesoscopic inhomogeneities *Phys. Rev. E* **80** 026123
- [18] Maslov S, Sneppen K and Zaliznyak A 2004 Detection of topological patterns in complex networks: correlation profile of the internet *Physica A* **333** 529
- [19] Park J and Newman M E J 2003 Origin of degree correlations in the internet and other networks *Phys. Rev. E* **68** 026112
- [20] Klemm K and Eguiluz V M 2002 Highly clustered scale-free networks *Phys. Rev. E* **65** 036123
- [21] Serrano M A and Boguná M 2005 Tuning clustering in random networks with arbitrary degree distributions *Phys. Rev. E* **72** 036133
- [22] Vázquez A 2003 Growing network with local rules: preferential attachment, clustering hierarchy, and degree correlations *Phys. Rev. E* **67** 056104
- [23] Huberman B A and Adamic L A 1999 Growth dynamics of the world-wide web *Nature* **401** 131
- [24] Mitrović M and Tadić B 2010 Bloggers behavior and emergent communities in blog space *Eur. Phys. J. B* **73** 293
- [25] Dankulov M M, Melnik R and Tadić B 2015 The dynamics of meaningful social interactions and the emergence of collective knowledge *Sci. Rep.* **5** 1

- [26] Liu J, Li J, Chen Y, Chen X, Zhou Z, Yang Z and Zhang C-J 2019 Modeling complex networks with accelerating growth and aging effect *Phys. Lett. A* **383** 1396
- [27] Pham T, Sheridan P and Shimodaira H 2016 Joint estimation of preferential attachment and node fitness in growing complex networks *Sci. Rep.* **6** 32558
- [28] Sen P 2004 Accelerated growth in outgoing links in evolving networks: deterministic versus stochastic picture *Phys. Rev. E* **69** 046107
- [29] Dorogovtsev S N and Mendes J F F 2001 Effect of the accelerating growth of communications networks on their structure *Phys. Rev. E* **63** 025101
- [30] Mitrović M and Tadić B 2012 *Emergence and Structure of Cybercommunities (Springer Optimization and Its Applications)* vol 57 (Berlin: Springer) p 209
- [31] Kantelhardt J W, Zschiegner S A, Koscielny-Bunde E, Havlin S, Bunde A and Stanley H E 2002 Multifractal detrended fluctuation analysis of nonstationary time series *Physica A* **316** 87
- [32] Mitrović M, Paltoglou G and Tadić B 2011 Quantitative analysis of bloggers' collective behavior powered by emotions *J. Stat. Mech.* **P02005**
- [33] Tadić B, Dankulov M M and Melnik R 2017 Mechanisms of self-organized criticality in social processes of knowledge creation *Phys. Rev. E* **96** 032307
- [34] Tadić B and Šuvakov M 2013 Can human-like bots control collective mood: agent-based simulations of online chats *J. Stat. Mech.* **P10014**
- [35] Hajra K B and Sen P 2004 Phase transitions in an aging network *Phys. Rev. E* **70** 056103
- [36] Schieber T A, Carpi L, Díaz-Guilera A, Pardalos P M, Masoller C and Ravetti M 2017 Quantification of network structural dissimilarities *Nat. Commun.* **8** 1
- [37] Sarigöl E, Pfitzner R, Scholtes I, Garas A and Schweitzer F 2014 Predicting scientific success based on coauthorship networks *EPJ Data Sci.* **3** 9
- [38] Myers S A and Leskovec J 2014 The bursty dynamics of the twitter information network *Proc. 23rd Int. Conf. on World Wide Web* 913
- [39] Smiljanić J and Dankulov M M 2017 Associative nature of event participation dynamics: a network theory approach *PloS One* **12** e0171565
- [40] Šuvakov M, Mitrović M, Gligorijević V and Tadić B 2013 How the online social networks are used: dialogues-based structure of MySpace *J. R. Soc. Interface* **10** 20120819
- [41] Peng C-K, Buldyrev S V, Havlin S, Simons M, Stanley H E and Goldberger A L 1994 Mosaic organization of DNA nucleotides *Phys. Rev. E* **49** 1685
- [42] Kantelhardt J W, Koscielny-Bunde E, Rego H H A, Havlin S and Bunde A 2001 Detecting long-range correlations with detrended fluctuation analysis *Physica A* **295** 441
- [43] Fürst EAFI Ihlen E A 2012 Introduction to multifractal detrended fluctuation analysis in Matlab *Front. Physiol.* **3** 141
- [44] Wever R A 2013 *The Circadian System of Man: Results of Experiments under Temporal Isolation* (Berlin: Springer)
- [45] Dorogovtsev S N and Mendes J F F 2001 Scaling properties of scale-free evolving networks: continuous approach *Phys. Rev. E* **63** 056125
- [46] Orsini C *et al* 2015 Quantifying randomness in real networks *Nat. Commun.* **6** 8627
- [47] Tian L, Zhu C-P, Shi D-N, Gu Z-M and Zhou T 2006 Universal scaling behavior of clustering coefficient induced by deactivation mechanism *Phys. Rev. E* **74** 046103
- [48] Gagen M J and Mattick J S 2005 Accelerating, hyperaccelerating, and decelerating networks *Phys. Rev. E* **72** 016123